

# Additional File 1

## for

E. Pasquier and R. J. Wellinger

*In vivo* chromatin organization on native yeast telomeric regions is independent of a cis-telomere loopback conformation.

- 6 Supplemental Figures
- Legends to the Supplemental Figures

### Fig. S1

**Chromatin organization of terminal Y' elements.** **a** Features identified on terminal portions of Y' elements, starting at the conserved XhoI site. Sequences from all Y' chromosomal ends (17/32) were analyzed and potential binding sites for Tbf1 and Reb1 proteins determined. Position of ACS is included. \*, incomplete sequencing data available at the very distal tip, the end of sequencing data is indicated by the end of the horizontal line. **b** Distances between MNase-sensitive sites identified in Fig. 1d. A size greater than 146 bp is compatible with positioning of a nucleosome, indicated by a dotted line. **c, d** Efficiency of cleavage by MNase-fused proteins on whole genomic DNA. Ethidium bromide staining of XhoI digested genomic DNA - related to Fig. 1c in **c**; and to Fig. 1b in **d**. Time of MNase activity in minutes and MNase-fused proteins are indicated on top of gels. Mono-, di-, tri-, tetra- refer to DNA sizes consistent with mono-, di- tri- and tetra-nucleosomes. M: DNA size marker.

### Fig. S2

**Chromatin organization of the terminal TEL03L X element.** Top: schematic drawing of XY' telomeres (left) and X-only telomeres (right) with positions of XhoI sites. The TG-repeat specific probe used is represented by a solid black line. TRF: Terminal Restriction Fragment. Bottom, autoradiograms of the blots shown in Figs. 1b and 1c as re-hybridized to the TG-repeat specific probe.

### Fig. S3

**Chromatin organization of the terminal TEL06R X element.** **a** Features identified on all terminal X elements, with respect to their start site. Sequences from X elements of X-only chromosomal ends were analyzed and potential binding sites of Tbf1 and Reb1 determined. Position of ACS is included. The end of X element is indicated by the end of the horizontal line. **b** Analysis of distances between MNase-sensitive sites. Size greater than 146 bp is compatible with positioning of a nucleosome, displayed by a dotted line. **c** related to Fig. 3c and 2b, plot profile of indicated strains. Y axis: Distance (cm), X axis: Intensity signal by pixels (% of total signal). (M) profiles are marker lanes.

### Fig. S4

**Chromatin organization of subtelomeric elements is independent of telomere length.** **a** Related to Fig. 4a; **b** related to Fig. 4b.; plot profiles of signal intensities obtained with *YKU80* and *yku80Δ* strains. Y axis: Distance (cm), X axis: Intensity signal by pixels (% of total signal). Telomeric area analyzed is indicated on top. Note that the shift to smaller size of the full TRF peak in the *yku80Δ* cells (see gray lines vs black lines) is fully expected as it corresponds to the short telomeric repeat tracts left in *yku80Δ* cells.

### Fig. S5

**Chromatin organization of X element from XY' chromosomal ends.** **a** Features identified on all X-elements of XY' junctions. Location of the ACS is included. The end of the X element is indicated by the end of the horizontal line. **b** Comparison of cut-sites is plotted with respect to a terminal X (TEL03L) versus an X of an XY' junction (TEL05R). Location of features (ACS, Abf1, Rap1, Tbf1 and Reb1 potential binding sites) are included. **c** Schematic drawing of TEL16R with the position of BamHI and XhoI sites. TEL16R specific probe used in **d** is represented by a solid black line. AF: Analyzed Fragment. **d** *In vivo* ChEC experiments with GBD-MN, NLS-MN and MN-

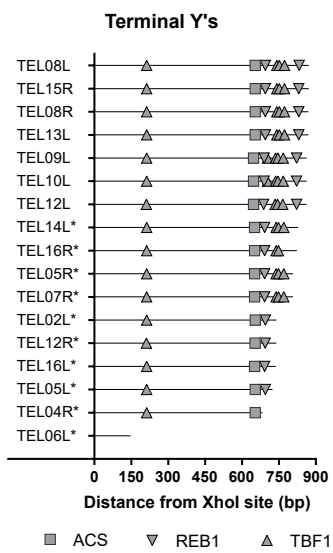
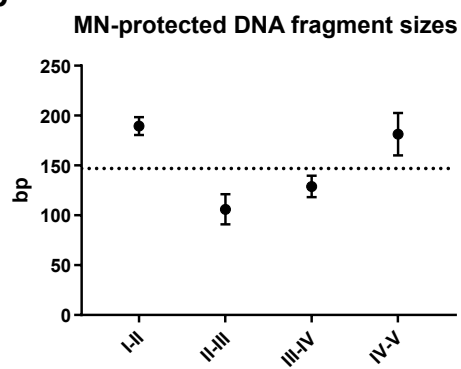
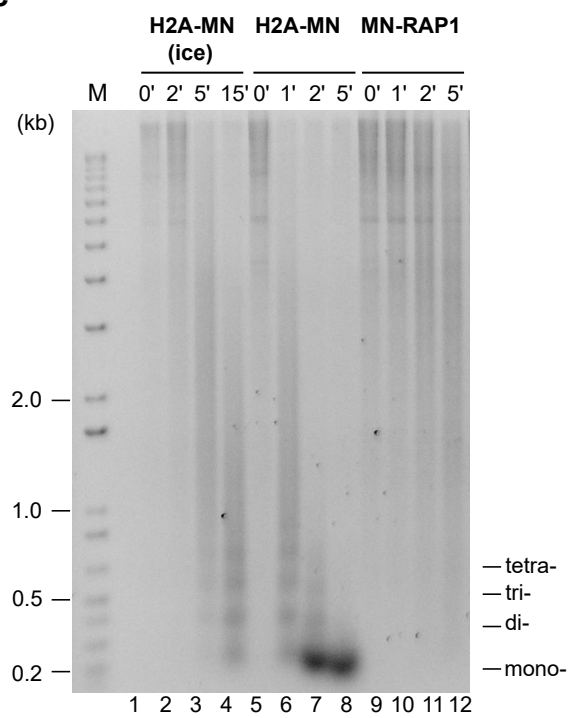
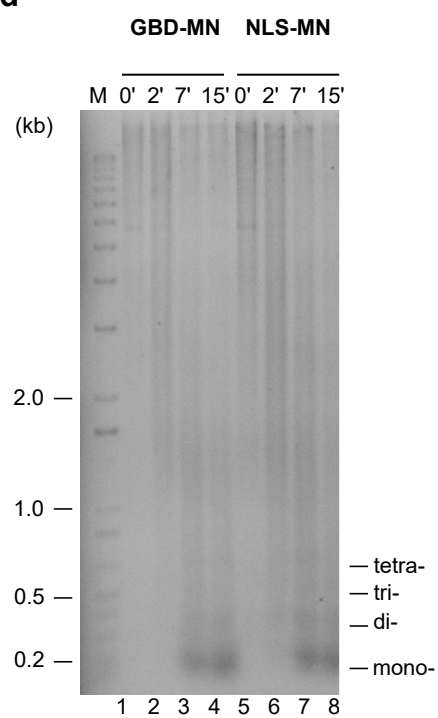
RAP1 analyzed on X element from TEL16R. Southern blot with BamHI and XhoI-digested genomic DNA hybridized to the TEL16R specific probe. Time of MNase activity in minutes is indicated on top of gels. Arrowheads with solid line indicate detectable cutting common to all MNase-fused proteins. **e** Location of MNase-sensitive sites on the TEL16R XY' junction. Position of features (ACS, Abf1, Rap1, Tbf1 and Reb1 potential binding sites) is included.

### Fig. S6

**No evidence of a stable telomere foldback structure by *in vivo* ChEC.** **a** Same *in vivo* ChEC as in Fig. 5b on the PvuI fragment of TEL05R obtained with Yku70-MN from *SIR4* (MVY221) and *sir4Δ* (MVL047) strains. **b** Analysis of Reb1 binding on TEL08L from SLIM-ChIP (short-fragment-enriched, low-input, indexed MNase ChIP) previously published (Gutin et al. 2018) **c** Potential binding sites of Rap1 on X-only chromosomal ends. Sequences from X-only chromosomal ends were analyzed and potential binding sites of Rap1 determined. **d** Same as in **c** but analysis was done on the telomere distal X elements of XY' chromosomal ends. Note that the clusters of Rap1 binding sites in the XY'-junction of the TEL13L, TEL12R, TEL14L, TEL12L, TEL06L, TEL04R and TEL08R are due to remaining telomeric TG<sub>1-3</sub> sequences between the X and Y' elements.

### Reference

Gutin, Jenia, Ronen Sadeh, Nitzan Bodenheimer, Daphna Joseph-Strauss, Avital Klein-Brill, Adi Alajem, Oren Ram, and Nir Friedman. 2018. "Fine-Resolution Mapping of TF Binding and Chromatin Interactions." *Cell Reports* 22 (10): 2797–2807. <https://doi.org/10.1016/j.celrep.2018.02.052>.

**Fig. S1****a****b****c****d**

**Fig. S2**

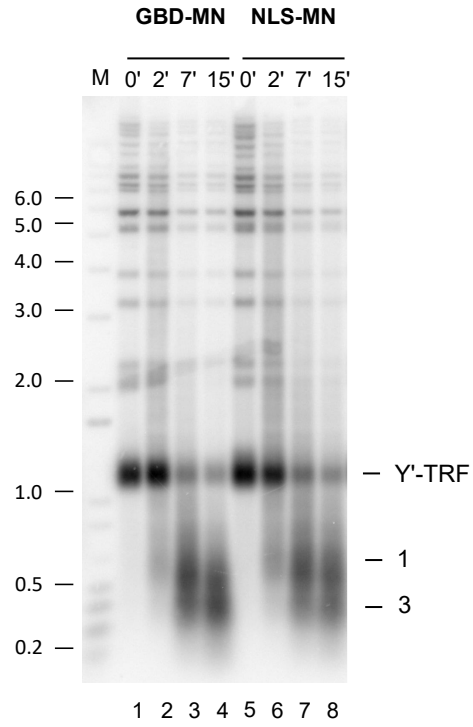
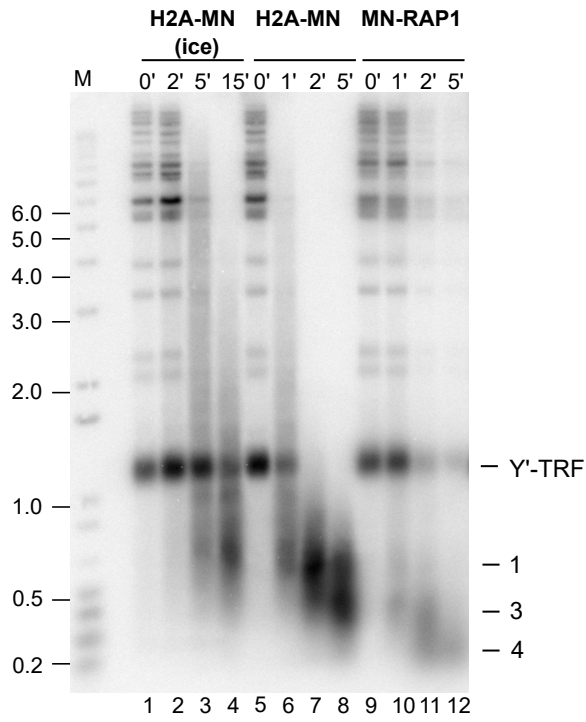
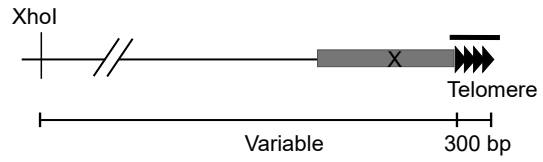
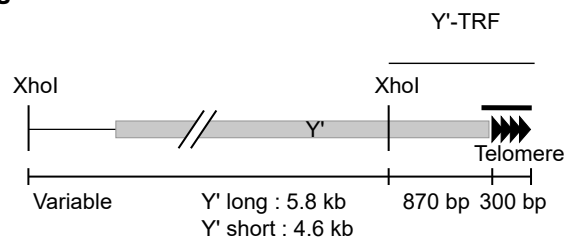
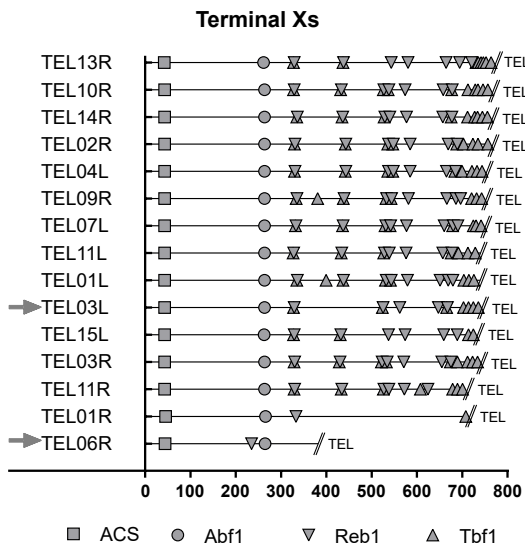
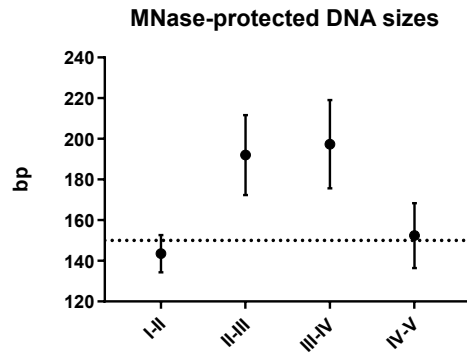


**Fig. S3**

**a**



**b**



**c**

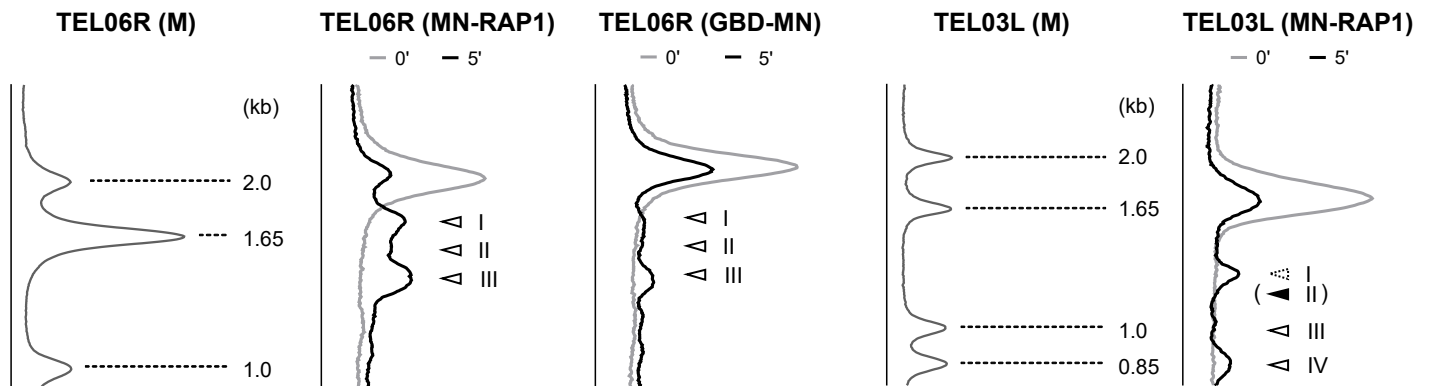
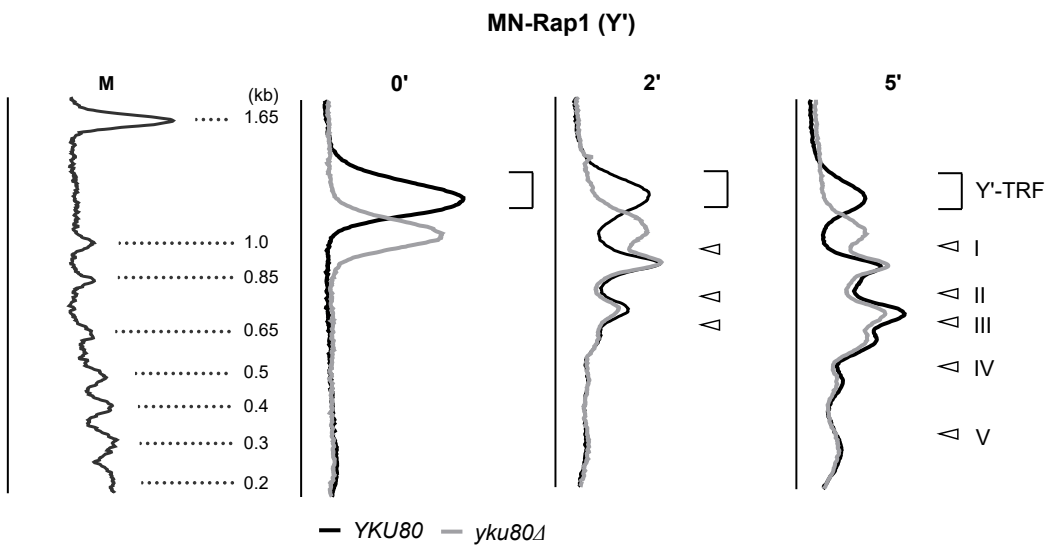


**Fig. S4**

**a**



**b**

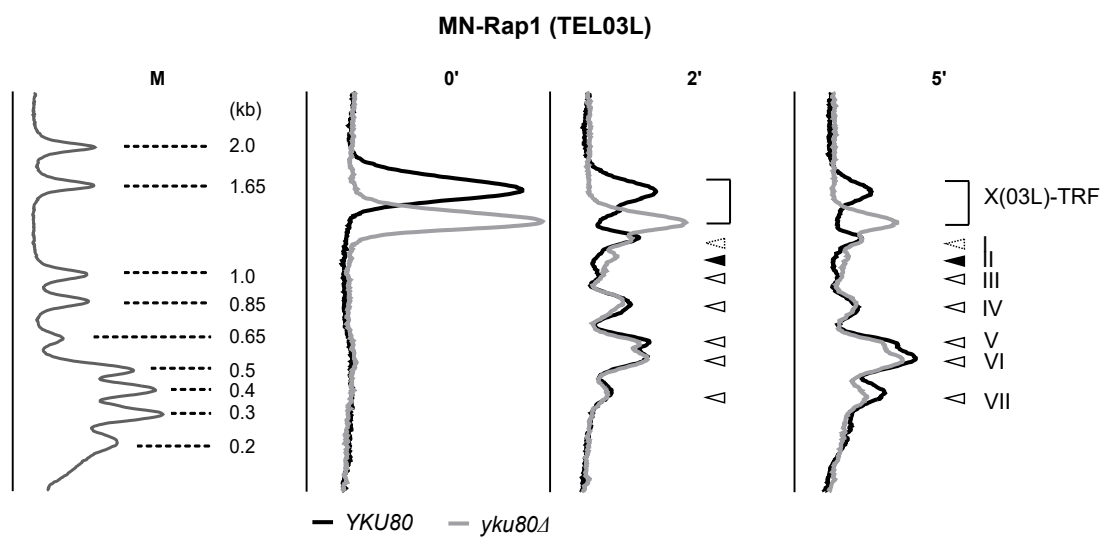
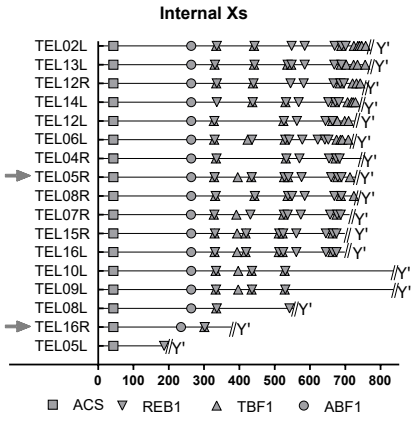
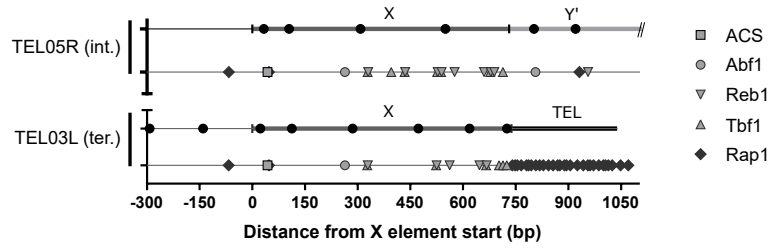


**Fig. S5**

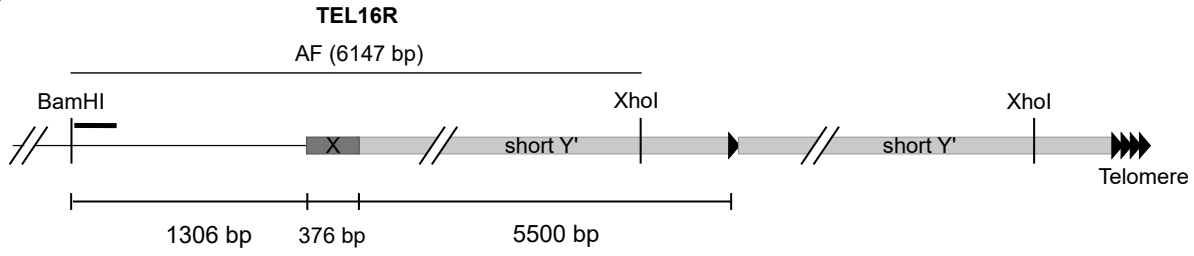
**a**



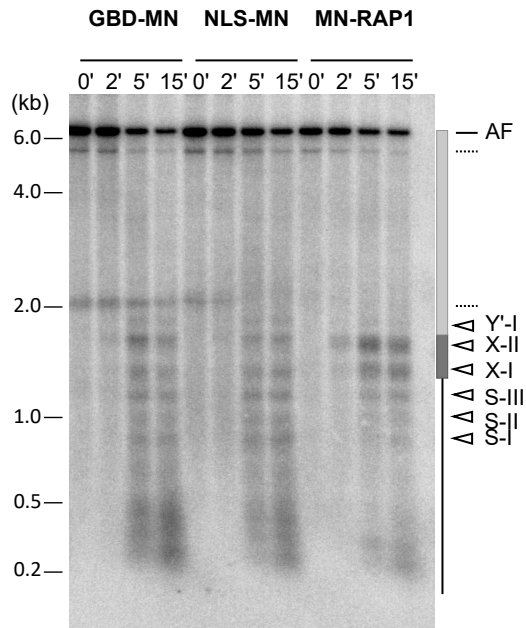
**b**



**c**



**d**



**e**

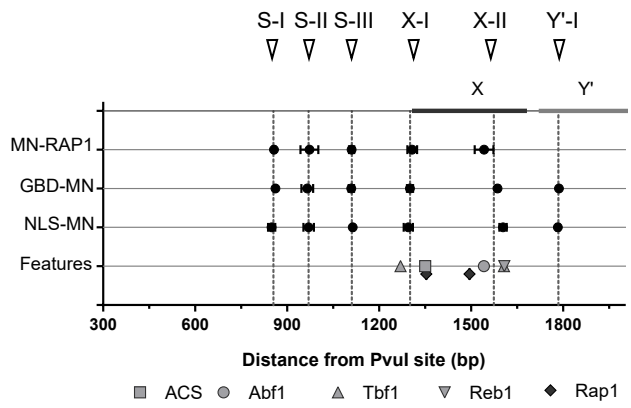




**Fig. S6**

